

Information theory based Electron Paramagnetic Resonance dating

C. Tannous¹ and J. Gieraltowski²

¹*Université de Brest, Lab-STICC, CNRS-UMR 6285, F-29200 Brest, FRANCE*

²*Laboratoire des Domaines Océaniques (IUEM), CNRS-UMR 6538, Technopôle Brest IROISE 29280 Plouzané, FRANCE*

(Dated: 20 June 2022)

Dating with Electron Paramagnetic Resonance (EPR) is based on exploiting effects of contamination by chemicals or ionizing radiation, on ancient matter through its absorption spectrum and lineshape. Interpreting absorption spectra as probability density functions (pdf), we introduce an Information Theory distance positioning the measured lineshape with respect to standard limiting pdf's (Lorentzian and Gaussian) allowing us to perform dating when several interaction possibilities between unpaired spins are present in ancient matter namely classical dipolar or quantum exchange coupling.

PACS numbers: 87.80.Lg, 76.30.-v, 75.30.Et, 75.40.Gb

Keywords: ESR/EPR techniques, EPR spectra in condensed matter, exchange interactions, spin diffusion

EPR (or ESR for Electron Spin Resonance) absorption spectroscopy is a non-interfering versatile technique that allows to explore interaction between unpaired spins (pertaining to electrons or holes in semiconducting solids) and an applied magnetic field in condensed matter. CW-EPR (Continuous wave) method measures concentrations of paramagnetic centers and free radicals by shining a sample with microwaves at a fixed frequency while simultaneously sweeping the magnetic field.

EPR provides precious information about local structures and dynamic processes of the paramagnetic centers within the sample under study.

Different frequencies are used such as S band (3.5 GHz), X band (9.25 GHz), K band (20 GHz), Q band (35 GHz) and W band (95 GHz). Each frequency has its own advantages and drawbacks and increasing it might increase its sensitivity. The latter is the minimal concentration of unpaired spins EPR can detect. For instance, going from the X to W band may result into a 30,000 enhancement in sensitivity. Since X band static sensitivity is around 10^{12} spins/cm³ this means the detection limit is decreased to 3.33×10^7 spins/cm³. Other means for improving static and dynamic sensitivity (in spins/Gauss/ $\sqrt{\text{Hz}}$) involve reducing temperature or miniaturizing experimental parts such as the resonant cavity or even employing cQED (circuit Quantum Electrodynamics) devices such as Josephson junctions, and SQUIDS, potentially reaching single-spin sensitivity by using high quality factor superconducting microresonators along with Josephson Parametric Amplifiers².

Importance of interest in EPR absolute dating capabilities stemmed from the fact ionizing radiation (α , β and γ) creates unpaired spins that might have extremely long lifetimes in certain materials³. Ionizing radiation originates from the fact rocks, sediments, minerals and deposits contain radioactive elements, such as potassium and isotopes produced by the ²³⁸U (Uranium), ²³⁵U (Actinium) and ²³²Th (Thorium) decay series.

Thus radiometric dating is based on accurate dosimetry estimation, that is how much any sample was exposed to ionizing radiation (or by extension to other

processes) tying the dose absorbed by the sample to its age. More precisely, the EPR signal intensity is proportional to the paleodose D (total radiation dose) given by $D = \int_0^T D_R(t) dt$ where $D_R(t)$ is the natural dose rate (in Grays/year) and T the exposure time or estimated age^{4,5}.

It is important to realize that EPR spectroscopy can handle radiometric dating as well as chemical dating that delivers information about various chemical processes a mineral has been subjected to¹.

While several other dating methodologies exist (see for instance Geyh and Schleicher⁶ or Ikeya's book⁴), the interest in EPR dating grew considerably after realizing its wide time range since it spans from a few thousand years to several million years and even billions which is far beyond capabilities of ¹⁴C dating (limited to about 50,000 years) for instance and allows to study geochronology since the formation of the Earth (about 4.5 billion years) until present time.

Historically Zeller⁷ suggested for the first time in 1968 the use of EPR for dating geological materials. In 1975 Ikeya⁴ was able to successfully date stalactite in Japanese caves with EPR and in 1978 Robins⁸ was even capable of identifying ancient heat treatment on flint artefacts with EPR.

More recently, Bourbin *et al.*⁶ and Gourier *et al.*¹⁰ introduced a statistical approach based on estimating an average area separating any given lineshape and the limiting Lorentzian (or Breit-Wigner). This measure is a statistical correlation factor called R_{10} that we show has several drawbacks and limitations. This is why we turn to Information Theory (IT) based distances called divergence measures that are able of tackling most of the cases a simple R_{10} correlation factor is unable to approach.

This work is organized as follows: After describing EPR spectroscopy and spin interactions classified as dipolar or exchange, we discuss the EPR lineshapes arising in both situations then move on to the dating procedure based on the evaluation of a statistical correlation factor R_{10} . The latter is unable to describe several

important cases (quantum exchange spin interaction or Gaussian pdf.). Thus we move on to introducing powerful IT tools based on evaluating distances (divergence measures) between pdf's originating from the EPR lineshape by integrating it with respect to the magnetic field and comparing IT results to R_{10} results when available. We do not address dosimetry procedures since this is beyond the goal of this work assuming that dosimetry has been tackled properly by other works.

EPR absorption spectroscopy reveals time-dependent interactions between electronic spins carrying magnetic moments in a material as reflected in the correlation function $S(t)$ also called Free Induction Decay function.

In general, a spin system is expected to interact (in a simplified manner) in two distinct ways:

1. When electrons are far apart i.e. $r \gg$ Angström (i.e. several hundred Angströms, microns and beyond) they can be considered as magnetic moments interacting in a magnetostatic fashion as $\frac{1}{r^3}$. This dipolar interaction¹¹ is considered as classical.
2. Quantum exchange¹² if spins are very close (typical nearest neighbour distance about a few Angströms). When electrons are close, overlap of their wavefunctions leads to short-range Slater interaction of the form $\exp(-r/r_0)$ with r the average inter-spin distance and r_0 on the order of an Angström.

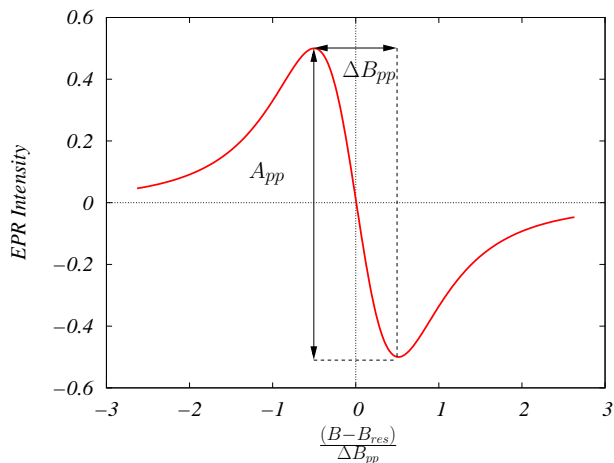


FIG. 1. (Color on-line) EPR lineshape key parameters: B_{res} resonance field, A_{pp} peak-to-peak amplitude and corresponding linewidth ΔB_{pp} .

The EPR lineshape is the field derivative of $S(t)$ Fourier Transform (FT).

In EPR or other resonance methods such as ferromagnetic (FMR) or nuclear magnetic resonance (NMR), there are, in general, two spin relaxation times: longitudinal T_1 (along applied external magnetic field) and transverse T_2 (perpendicular to applied external

magnetic field).

In the dipolar¹¹ case, Fel'dman and Lacelle¹³ have shown that spin correlation function is given by:

$$S(t) = S(0) \exp[(-t/T_2)^\beta] \quad (1)$$

with T_2 the transverse relaxation time, a measure of spin density in the sample and $\beta = \frac{D}{3}$ with D the dimension of geometrical spin arrangement (3 for full spatial, 2 for layers or thin films and 1 for spin chains).

In the $D = 3$ dipolar case, $\beta = 1$ and $S(t) = S(0) \exp[-t/T_2]$ whose FT is a Lorentzian $\hat{S}(\Delta\omega) = \frac{1}{\pi} \frac{T_2}{[1+(\Delta\omega T_2)^2]}$ where $\Delta\omega$ is frequency difference with respect to resonance frequency.

In EPR spectroscopy, the Lorentzian and the Gaussian absorption curves are considered as limiting absorption curves whose derivatives with respect to the applied field yields the EPR lineshape.

A Lorentzian appears when we have homogeneous broadening whereas a Gaussian results (in a solid) from thermal fluctuations of atomic/ionic constituents causing changes in the local magnetic field (cf Jonas review⁵).

Magnetic resonance is such that frequency $\omega = \gamma B$ where γ is gyromagnetic ratio given by $\gamma = \mu_0 g_L e \hbar / 2m_e$ (μ_0 = vacuum permeability, g_L = Landé factor, e, m_e = charge and electron mass).

This implies $\Delta\omega \propto B - B_{res}$ with B (applied field) and resonance field B_{res} .

The $S(t)$ FT is a Lorentzian in B such that: $\hat{S}(B) = \frac{1}{\pi} \frac{1}{[1 + (\frac{B - B_{res}}{\Delta B_{pp}})^2]}$.

The EPR lineshape is obtained by taking the derivative with respect to applied field B of $\hat{S}(B)$ such that $F(B) = \frac{d\hat{S}(B)}{dB}$. Note that $\hat{S}(B)$ is often denoted as the EPR power absorption, the imaginary part of the generalized susceptibility $\chi''(B)$.

At lower dimensionality $D = 1, 2$ the rational exponent $\frac{D}{3}$ leads to a "stretched exponential", "stretched Gaussian" or even "stretched Lorentzian" dependence (cf fig 2 and note¹⁴).

Thus "stretched" refers to a spatial arrangement of spins in planes or layers ($D = 2$) or along linear chains ($D = 1$).

To summarize, $\beta = 1$ yields a pure exponential with Lorentzian FT, whereas when $\beta = 2$ we obtain a Gaussian with a Gaussian FT and for intermediate values $1 < \beta < 2$, we recover the stretched curve varieties.

$S(t)$ FT is written as $\hat{S}(\omega) = \int_0^{+\infty} e^{-i\omega t} S(t) dt$.

In EPR, ω is proportional to the applied magnetic field allowing us to replace ω by $B - B_{res}$ resulting in $\hat{S}(B - B_{res}) = \int_0^{+\infty} e^{-ia(B-B_{res})t} S(t) dt$ with $a = g_L \mu_B / \hbar$, g_L the Landé factor, μ_B Bohr magneton and \hbar Planck constant.

EPR lineshape $F(B)$ is obtained from the derivative with respect to B of $\hat{S}(B - B_{res})$ yielding:

$$\begin{aligned} F(B) &= Re \left[\int_0^{+\infty} \frac{d}{dB} e^{-ia(B-B_{res})t} S(t) dt \right] \\ &= -a \int_0^{+\infty} t \sin[a(B - B_{res})t] S(t) dt \end{aligned} \quad (2)$$

Hence it suffices to evaluate the above integral using $S(t) = S(0) \exp[(-t/T_2)^{\frac{D}{3}}]$ and $D = 1, 2, 3, 6$ to recover the stretched Lorentzian ($D = 1, 2$) (cf note¹⁴), the Lorentzian ($D = 3$) and finally the Gaussian ($D = 6$).

Integrating requires special methods to reduce errors resulting from large number of oscillations emanating from the term $\sin[a(B - B_{res})t]$. Moreover one has to determine from the lineshape A_{pp} and ΔB_{pp} depending on D, T_2, a (cf. fig. 1).

EPR lineshape results displayed in fig. 2 show that we evolve from Gaussian to Lorentzian ($D = 3$), to stretched Lorentzian ($D = 2$) and finally stretched Lorentzian ($D = 1$). Comparing to the quantum or "spin diffusion" case (fig. 3) based on spin correlation function $S(t) = S(0) \exp[(-t/T_2)^{\beta(D)}]$ with $\beta(D)$ function of dimensionality D . $\beta = 3/2$ in 1D (see Dietz *et al.*¹⁵) and $\beta = 1$ in 2D (a simplified version of the very complex 2D case (see Richards *et al.*¹⁶)).

Classical dipolar interactions lead to spectrum broadening¹⁷ i.e. damping. In sharp contrast, quantum exchange among spins tends to reduce the EPR linewidth ("Exchange Narrowing" effect) and consequently, damping.

Characterizing the EPR lineshape around resonance, Bourbin *et al.*⁶ and Gourier *et al.*¹⁰ introduced a statistical method based on an average area estimation between any given lineshape and the 3D Lorentzian.

They introduced after ref.^{15,16} functional transformations $B \rightarrow x$ and $F(B) \rightarrow f(x)$ (function $F(B)$ is the derivative with respect to magnetic field of the $S(t)$) FT with definitions:

$$\begin{aligned} x &= \left(\frac{B - B_{res}}{\Delta B_{pp}} \right)^2, \\ y = f(x) &= \sqrt{\frac{A_{pp}}{|F(B - B_{res})|} \frac{|B - B_{res}|}{\Delta B_{pp}}} \end{aligned} \quad (3)$$

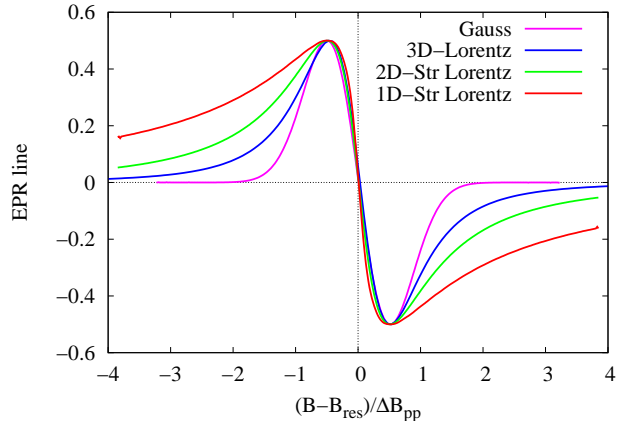


FIG. 2. (Color on-line) Illustration of dipolar broadening with EPR lineshapes corresponding to spin correlation function $S(t) = S(0) \exp[(-t/T_2)^{\frac{D}{3}}]$ for a fixed value of parameter A_{pp} . The Gaussian profile is the narrowest then we progress toward the broader Lorentzian ($D = 3$), stretched Lorentzian ($D = 2$) and finally the ($D = 1$) stretched Lorentzian. **Note:** Str means Stretched.

Thus "Lorentzian derivative" $F(B)$ corresponds to linear function $f_L(x) = x + 3/4$ whereas "Gaussian derivative" corresponds to $f_G(x) = \exp(x - 1/4)$. Then a correlation factor R_{10} is extracted with:

$$R_{10} = \frac{1}{10} \int_0^{10} [f(x) - f_L(x)] dx \quad (4)$$

meaning that the area estimation is some kind of distance measure separating the lineshape from the Lorentzian; in addition R_{10} is equal to zero when $f(x) = f_L(x)$.

When $R_{10} > 0$ we have close-neighbour spins regime (quantum exchange interaction) with a mixed Gaussian-Lorentzian profile.

Finally, when $R_{10} < 0$ we have distant spins (dipolar regime) in lower dimension ($D = 1, 2$) with a stretched Lorentzian lineshape.

In the dipolar case, $x, f(x)$ diagrams (cf fig. 4) serve to identify $R_{10} > 0$ region between Gaussian and Lorentzian whereas $R_{10} < 0$ is below the Lorentzian.

In sharp contrast, $x, f(x)$ diagrams in the exchange case for $D = 1, 2$ (region $R_{10} > 0$) are between the Lorentzian and the Gaussian (cf fig. 5). Thus one has to distinguish the classical dipolar from the quantum exchange case when encountering $R_{10} > 0$.

Nevertheless, obtaining R_{10} from EPR lineshape is interesting since it allows determination of the nature of spin interactions as quantum or classical (from $S(t)$) and their geometrical arrangement from the D value as done

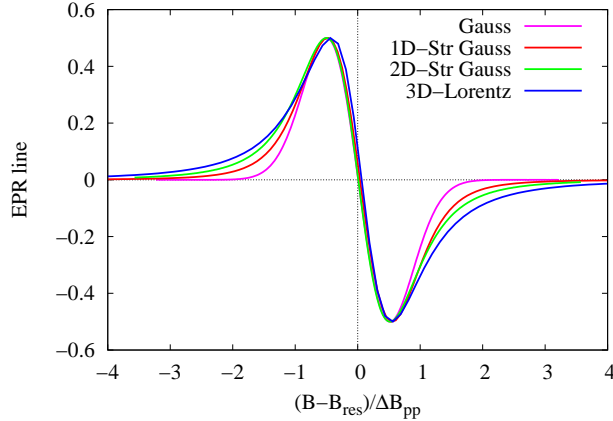


FIG. 3. (Color on-line) Illustration of exchange narrowing with EPR lineshapes derived from $S(t) = S(0) \exp[(-t/T_2)^{\beta(D)}]$ with $\beta(D)$ function of dimension D . Lineshapes evolve to broader (Stretched) from narrowest (Gaussian) as dimensionality increases ($D = 1, 2, 3$) in sharp contrast with respect to the dipolar case (fig. 2). When $D = 3$ the Lorentzian is recovered as in the dipolar case.

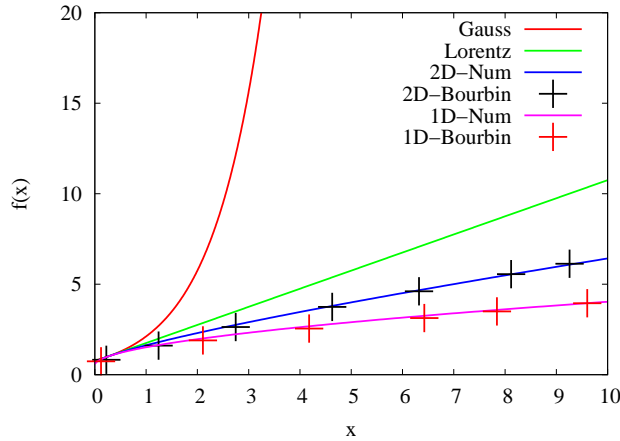


FIG. 4. (Color on-line) $f(x)$ functions corresponding to the different $F(B)$. "Lorentzian derivative" corresponds to $f_L(x) = x + 3/4$ whereas "Gaussian derivative" corresponds to $f_G(x) = \exp(x - 1/4)$. Our results agree with Bourbin *et al.*⁶ numerical calculations.

by Bourbin *et al.*⁶ and Gourier *et al.*¹⁰ who considered only the classical dipolar case $D = 1, 2$, thus the need to examine the quantum picture (cf fig. 3).

In the intermediate dipolar case (lower dimensionality) $D = 1, 2$ lines are under the Lorentzian, whereas in the intermediate exchange^{15,16} case $D = 1, 2$ lines are between the Gaussian and the Lorentzian.

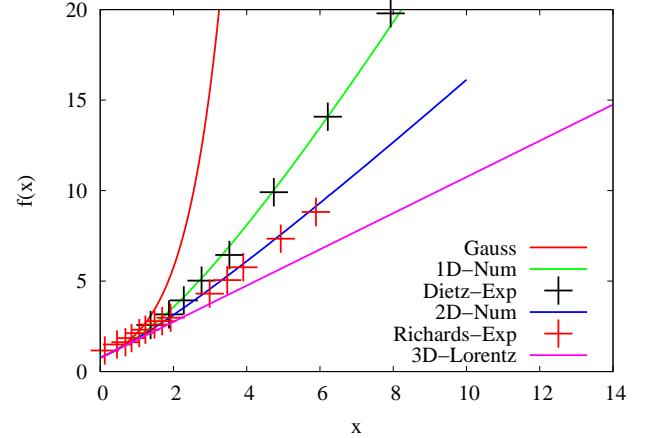


FIG. 5. (Color on-line) In the quantum case $D = 1, 2$ curves lie between the Lorentzian and the Gaussian and our results agree with experimental data of Dietz *et al.*¹⁵ in 1D for $(\text{CH}_3)_4\text{NMnCl}_3$ as well as with Richards *et al.*¹⁶ in 2D for K_2MnF_4 .

Note: Num stands for numerical and Exp for experimental.

This is important in order to obtain a reliable and precise dating assessment of rocks and sediments along the lines of Bourbin *et al.*⁶ and Gourier *et al.*¹⁰ who derived two different sets of age formulae from the R_{10} factor.

Introducing a measure based on Information Theory¹ helps to discriminate between the classical and quantum pictures.

There are several divergence or distance measures between probability densities such as the Kullback-Leibler^{1,3}, squared Hellinger, α -divergence, Jensen-Shannon, total variation^{1,20}... (see Supplementary Material).

We choose the Cauchy-Schwarz divergence (CSD) measure^{1,3} defined between two probability distributions P, Q as:

$$D(P||Q) = -\ln \left(\int_{x \in \mathcal{X}} dx p(x)q(x) \right) + \frac{1}{2} \ln \left(\int_{x \in \mathcal{X}} dx p^2(x) \right) + \frac{1}{2} \ln \left(\int_{x \in \mathcal{X}} dx q^2(x) \right) \quad (5)$$

where \mathcal{X} is the set of values taken by continuous probability densities (pdf) $p(x), q(x), x \in \mathcal{X}$.

CSD obeys several axioms of distance (see Supplementary Material) such as positivity $D(P||Q) \geq 0$, and triangle inequality: $D(P||R) \leq D(P||Q) + D(Q||R)$. It obeys also symmetry $D(P||Q) = D(Q||P)$ unlike the Kullback-Leibler (KL) measure^{1,3} defined by:

$$D_{KL}(P||Q) = \int_{x \in \mathcal{X}} dx p(x) \ln \frac{p(x)}{q(x)} \quad (6)$$

Moreover CSD does not suffer from singularities whereas

KL does.

The pdf are obtained from the EPR lineshape by integrating it with respect to the magnetic field (Detailed procedure is described in Supplementary Material).

In Table I we display CSD distances between a unit Lorentzian pdf and a set of Dipolar and Exchange pdf along with the R_{10} factor and corresponding ages.

In Table II we display CSD distances between a unit Gaussian and a set of Dipolar and Exchange pdf along with the R_{10}^* factor and corresponding ages that would correspond to formula:

$$R_{10}^* = \frac{1}{10} \int_0^{10} [f(x) - f_G(x)] dx, f_G(x) = \exp(x - 1/4) \quad (7)$$

Actually, we did not use the above formula and rather extrapolated the Lorentzian R_{10} values to estimate the age by modifying Bourbin *et al.* coefficient α_B (age extraction procedure is explained in Supplementary Material).

Lorentzian P	$D(P Q)$	R_{10}	Age (Gyr)
Dipolar pdf Q			
$D = 1$ Str Lorentz	0.21	-2.94	3.54
$D = 2$ Str Lorentz	2.50×10^{-2}	-1.94	2.74
$D = 3$ Lorentz	1.19×10^{-6}	0.0	1.67
Gauss	2.55×10^{-2}	1.71×10^3	Undefined
Exchange pdf Q			
$D = 1$ Str Gauss	1.14×10^{-2}	6.78	0.29
$D = 2$ Str Gauss	4.12×10^{-3}	2.30	0.93
$D = 3$ Lorentz	1.19×10^{-6}	0.0	1.67
Gauss	2.55×10^{-2}	1.71×10^3	Undefined

TABLE I. Cauchy-Schwarz distances separating a unit width P Lorentzian and Q distributions (Dipolar and Exchange) with corresponding R_{10} factor yielding age in Gyr (billion years). Age in years is deduced from Bourbin *et al.*⁶ formula $10^{\left(\frac{R_{10} - \beta_B}{\alpha_B}\right)}$ with $\alpha_B = -9.$ and $\beta_B = 83.$. Note that Skrzypczak *et al.*¹⁰ define another set of coefficients: $\alpha_S = -5.3$ and $\beta_S = 48.9$ (Other examples are detailed in Supplementary Material).

In this work we developed an EPR lineshape based dating methodology handling both Dipolar (classical) and Exchange (quantum) interactions between unpaired spins.

It is based on evaluating IT distances (divergence measures) between a Lorentzian or a Gaussian pdf and an experimental pdf obtained from the measured EPR lineshape integrated over the applied magnetic field.

While aging is considered as bringing about a stretched exponential type pdf according to Fel'dman *et al.*¹³ (in the dipolar interaction case) whereas in the exchange interaction case, Dietz *et al.*¹⁵ and Richards *et al.*¹⁶ in-

Gaussian P	$D(P Q)$	R_{10}^*	Age (Myr)
Dipolar pdf Q			
$D = 1$ Str Lorentz	0.25	-2.94	90.59
$D = 2$ Str Lorentz	5.11×10^{-2}	-2.89	89.61
$D = 3$ Lorentz	1.51×10^{-2}	2.73	27.09
Gauss	0.0	0.0	48.44
Exchange pdf Q			
$D = 1$ Str Gauss	1.86×10^{-2}	-5.02×10^{-2}	48.96
$D = 2$ Str Gauss	1.44×10^{-2}	3.51	22.91
$D = 3$ Lorentz	1.51×10^{-2}	2.73	27.09
Gauss	0.0	0.0	48.44

TABLE II. Cauchy-Schwarz distances separating a unit standard deviation P Gaussian and Q distributions (Dipolar and Exchange). The corresponding R_{10}^* factor is obtained from extrapolating the above Lorentzian R_{10} value and the age obtained in Myr (million years) is deduced from altering the Bourbin *et al.* coefficient α_B (Other examples are detailed in Supplementary Material).

roduced another type of stretched exponential pdf, we consider in this work, aging as an IT distance between pdf's stemming from EPR lineshapes integrated with respect the applied magnetic field.

IT provides an alternate look at dating based on using special distances (with respect to Gaussian, Lorentzian...) as well as arbitrary coupling between spins (dipolar, exchange...) paving the way to cover any period of time with the proviso of having performed previously an appropriate dosimetry analysis.

- ¹Y. Pan, N. Chen, J. A. Weil and M. J. Nilges, *American Mineralogist*, **87**, 1331 (2002).
- ²S. Probst, A. Bienfait, P. Campagne-Ibarcq, J. J. Pla, B. Albanese, J. F. Da Silva Barbosa, T. Schenkel, D. Vion, D. Esteve, K. Mølmer, J. J. L. Morton, R. Heeres, and P. Bertet, *App. Phys. Lett.* **111**, 202604 (2017).
- ³A.R. Skinner, ESR dating: is it still an "experimental" technique? *Appl. Radiat. Isot.* **52** 1311 (2000).
- ⁴Ikeya, M., *Nature* **255** (1975) and "New Applications of Electron Spin Resonance: Dating, Dosimetry and Microscopy", edited by M. Ikeya, World Scientific Publishing, Singapore (1993).
- ⁵M. Jonas, *Concepts and Methods of ESR dating, Radiation Measurements*, Elsevier, **27**, 943 (1997).
- ⁶M. A. Geyh and H. Schleicher, "Absolute Age Determination Physical and Chemical Dating Methods and Their Application", Springer-Verlag, Berlin, (1990).
- ⁷E. J. Zeller, in "Thermoluminescence of Geological Materials", edited by D. J. McDougall, chapter 5.1, 271 and chapter 6.1 (Academic, London, 1968).
- ⁸G.V. Robins, N.J. Seeley, D.A.C. McNeil, and M.C.R. Symons, Identification of ancient heat treatment in flint artefacts by ESR spectroscopy, *Nature* **276**, 703 (1978).
- ⁹M. Bourbin, D. Gourier, S. Derenne, L. Binet, Y. Le Du, F. Westall, B. Kremer and P. Gautret: Dating carbonaceous matter in archean cherts by electron paramagnetic resonance, *Astrobiology* **13-2**, 151 (2013).
- ¹⁰A Skrzypczak-Bonduelle, L Binet, O Delpoux, H Vezin, S Derenne, F Robert and D Gourier: EPR of radicals in primi-

- tive organic matter: a tool for the search of biosignatures of the most ancient traces of life, *App. Magn. Reson.* **33**, 371 (2008).
- ¹¹J.H. Van Vleck, The dipolar broadening of magnetic resonance lines in crystals. *Phys Rev.* **74**, 1168 (1948).
- ¹²A. Bencini and D. Gatteschi, Exchange narrowing in lower dimensional systems, in "EPR of Exchange Coupled Systems" 155, Springer-Verlag, Berlin (1990).
- ¹³EB Fel'dman, S Lacelle: Configurational averaging of dipolar interactions in magnetically diluted spin networks, *J Chem Phys* **104** 2000 (1996).
- ¹⁴One might be tempted to believe since Lorentzian is $\frac{1}{\pi} \frac{1}{[1+x^2]}$, then a stretched Lorentzian would be $\frac{1}{[1+x^\alpha]}$ avec $\alpha > 2$ with $\alpha < 2$. In fact, a stretched Lorentzian curve has several meanings: one might have a superposition of Lorentzians or more complicated functions (possibly containing terms such as $\frac{1}{[1+x^\alpha] \dots}$). Generally, any function whose width is larger than the Lorentzian is considered stretched.
- ¹⁵R. E. Dietz, F. R. Merritt, and R. Dingle: Exchange Narrowing in One-Dimensional Systems, *Phys. Rev. Lett.* **26**, 1186 (1971).
- ¹⁶PM Richards and MB Salmon: Exchange Narrowing of electron spin resonance in a Two-Dimensional System, *Phys. Rev. B.* **9**, 32 (1974).
- ¹⁷C. Kittel and E. Abrahams, Dipolar broadening of magnetic resonance lines in magnetically diluted crystals. *Phys Rev* **90** 238 (1953).
- ¹⁸T. M. Cover, J. A. Thomas, "Elements of Information Theory" John Wiley and Sons, (1991)
- ¹⁹W.H. Press, S.A. Teukolsky, W.T. Vetterling and B.P. Flannery, "Section 14.7.2. Kullback-Leibler Distance", in "Numerical Recipes: The Art of Scientific Computing" (3rd ed.), Cambridge University Press (2007).
- ²⁰D. Morales, L. Pardo, M. Salicrù and M. L. Menéndez, *J. Stat. Planning and Inference* **38**, 201 (1994).

Supplemental Material to “Information theory based Electron Paramagnetic Resonance dating”

Information Theory (IT) provides a divergence measure or effective distance^{S1} separating two functions (in this case probability density functions or pdf) to enable their comparison not only from the geometrical shape point of view but also from the information content as well.

Going from a distance between two points to one between two functions helps determine how much the functions are dissimilar from several points of view (analytical, geometrical and informational). That is why $D(P||Q)$ is also called relative information entropy that does not behave as a metric but rather as the square of the Euclidian one^{S1}.

Several examples of $D(P||Q)$ are displayed in Table I.

Distance $D(P Q)$	Definition
Squared Hellinger	$\int_{x \in \mathcal{X}} dx (\sqrt{p(x)} - \sqrt{q(x)})^2$
Squared triangular	$\int_{x \in \mathcal{X}} dx \frac{(q(x)-p(x))^2}{p(x)+q(x)}$
Squared perimeter	$\int_{x \in \mathcal{X}} dx \sqrt{p^2(x) + q^2(x)} - \sqrt{2}$
α -divergence	$\frac{4}{1-\alpha^2} \left(1 - \int_{x \in \mathcal{X}} dx p^{\frac{1-\alpha}{2}}(x) q^{1+\alpha}(x) \right)$
Jensen-Shannon	$\frac{1}{2} \int_{x \in \mathcal{X}} dx \left(p(x) \ln \frac{2p(x)}{p(x)+q(x)} + q(x) \ln \frac{2q(x)}{p(x)+q(x)} \right)$
Pearson χ_P^2	$\int_{x \in \mathcal{X}} dx \frac{(q(x)-p(x))^2}{p(x)}$
Neyman χ_N^2	$\int_{x \in \mathcal{X}} dx \frac{(q(x)-p(x))^2}{q(x)}$
Total variation (metric)	$\frac{1}{2} \int_{x \in \mathcal{X}} dx p(x) - q(x) $

TABLE I. Examples of Information Theory distances or divergences between two pdf $p(x), q(x)$. Note that α -divergence, Pearson χ_P^2 and Neyman χ_N^2 do not satisfy the axiomatic symmetry requirement of a distance $D(P||Q) = D(Q||P)$.

The Cauchy-Schwarz divergence (CSD) measure^{S1,S3} is convenient since it obeys the axioms of distance and is free of singularities (see main article). Given two probability distributions P, Q the CSD measure is:

$$D(P||Q) = -\ln \left(\int_{x \in \mathcal{X}} dx p(x)q(x) \right) + \frac{1}{2} \ln \left(\int_{x \in \mathcal{X}} dx p^2(x) \right) + \frac{1}{2} \ln \left(\int_{x \in \mathcal{X}} dx q^2(x) \right) \quad (S1)$$

where \mathcal{X} is the set of values taken by continuous pdf $p(x), q(x), x \in \mathcal{X}$.

EPR absorption spectra when interpreted as a pdf (see fig. S1 for the Lorentzian case), is considered as modified by aging due to time-dependent interactions between electronic spins in a geological material. The time correlation function $S(t)$ (Free Induction Decay function) yields the EPR lineshape $F(B)$ since it is the field derivative of its Fourier Transform (FT).

Thus an IT distance could be used as a measure of aging induced by ionizing radiation and this supplement details and illustrates the procedure for carrying the dating method.

A. Experimental protocols

Experimentally, two procedures are possible:

1. Direct treatment of the absorption spectra considered as a pdf and evaluating the IT distance with respect to a given reference (Lorentzian, Gaussian...).
2. Extraction of the absorption spectra from the measured EPR lineshape $F(B)$ by integrating it with respect to the applied field B and afterwards evaluating the IT distance.

The extraction of the absorption spectrum from EPR lineshape $F(B)$ entails several steps:

1. Spline interpolation of the EPR lineshape $F(B)$.
2. Symmetrization of the EPR lineshape using shifting by δ such that $\int F(B)dB = \delta \int dB$.
3. Field integration of the symmetrized EPR lineshape to get the absorption spectrum.

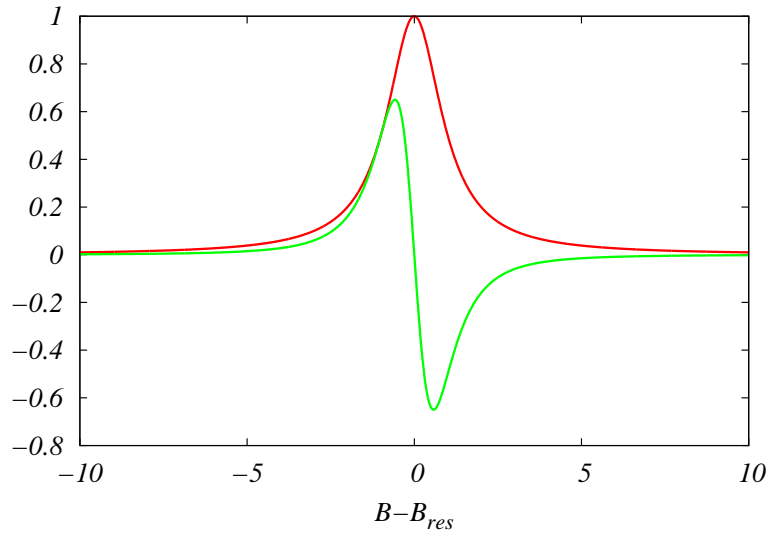


FIG. S1. (Color on-line) absorption line (in red) and its field derivative the EPR lineshape (in green) in the Lorentzian case.

4. Filtering (smoothing) of the absorption spectrum.

5. Normalization of the absorption spectrum and transformation into a pdf $p(x)$ with $x = \left(\frac{B - B_{res}}{\Delta B_{pp}} \right)$.

After transformation of the EPR lineshape into a pdf, the evaluation of the CSD divergence measure^{S1,S3} can be undertaken to determine the age from the evaluation of the CSD measure taken between the different probability distributions corresponding to the EPR spectrum and the Lorentzian or Gaussian considered as limiting distributions.

B. Age determination from CSD

Age is determined from (CSD) distances d_L and d_G with respect to unit Lorentzian and Gaussian distributions labelled as $p(x)$ as well as from σ_q the standard deviation of $q(x)$ corresponding to the measured EPR spectrum. Age is evaluated with the formula $10^{A_{L,G}}$ where $A_{L,G} = d_{L,G}^\xi \sigma_q^\eta$ for the Gyr (billion year), Myr (million year) cases whereas it is given by $A_{L,G} = d_{L,G}^\zeta \sigma_q^\eta$ for the Kyr (thousand year) cases with $d = d_L$ in the Lorentz or $d = d_G$ in the Gaussian case. Exponents $\xi = -1.28$, $\eta = 2.74 \times 10^{-2}$, $\zeta = -0.32$ are determined by optimization (see Table II).

Sample	d_L	d_G	σ_q	Lorentz Age	Gauss Age
Gunflint ^{S2}	0.18	0.23	8.17	2.34 Gyr	8.91×10^{-3} Gyr
B4 ^{S4}	0.21	0.21	0.77	8.51 Myr	11.78 Myr
Enamel ^{S5}	1.49×10^{-2}	1.17×10^{-2}	1.60	7.29 Kyr	14.47 Kyr

TABLE II. Age is evaluated with the formula $10^{A_{L,G}}$ where $A_{L,G} = d_{L,G}^\xi \sigma_q^\eta$ for the Gyr, Myr cases whereas it is given by $A_{L,G} = d_{L,G}^\zeta \sigma_q^\eta$ for the Kyr cases with $d = d_L$ for the Lorentz case or $d = d_G$ for the Gaussian case.

We illustrate the Information Theory dating procedure with a first example pertaining to Gunflint from Schreiber beach locality (Port Arthur Homocline) in Ontario Canada with age about 1.88 Giga-years according to Skrzypczak PhD thesis^{S2}.

After extracting the absorption spectrum from the EPR lineshape, we find the CSD between Skrzypczak Gunflint^{S2} $q(x)$ and a unit Lorentzian $p(x)$ as 0.18 whereas it is 0.23 between $q(x)$ and a unit Gaussian $p(x)$.

In order to extract the age based on the R_{10} evaluation explained in the main work to find: $R_{10} = -1.765$ with age=2.62 Giga-years. Lorentz and Gauss CSD ages are 2.34 Gyr and 8.91×10^{-3} Gyr respectively (cf. Table II) whereas Skrzypczak^{S2} estimated it to be 1.88 Giga-years.

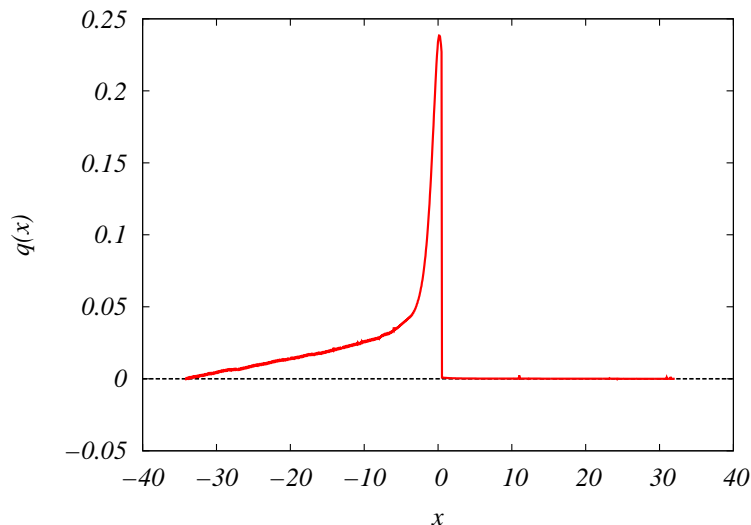


FIG. S2. (Color on-line) Absorption line obtained from the EPR lineshape Gunflint sample taken from Skrzypczak PhD thesis^{S2} fig.II.25

Another example is a latosol sediment called B4 drawn from Balan *et al.*^{S4} fig.2 and extracted from 100 cm depth at a site 60 km North of the city of Manaus capital of Amazonas state in North-Western Brazil.

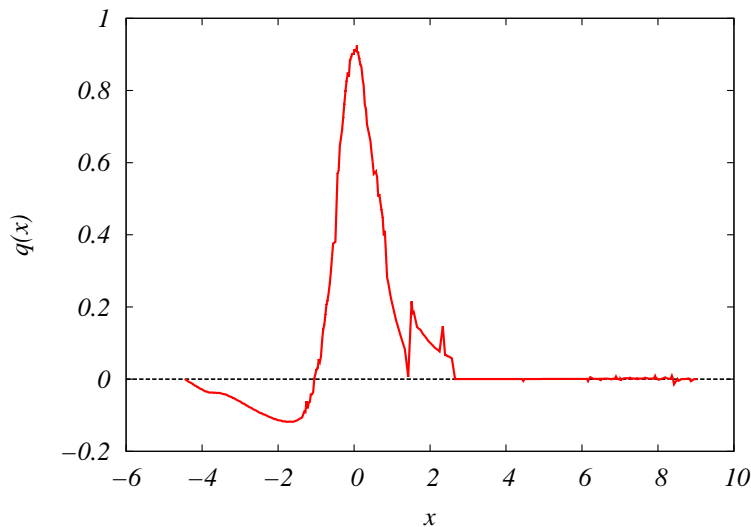


FIG. S3. (Color on-line) Absorption line obtained from the EPR lineshape B4 latosol sediment of Balan *et al.*^{S4} fig.2. The negative wing of the pdf is taken care of by upward shifting of the curve.

The age is determined from the R_{10} evaluation obtained as $R_{10} = -0.575$ with age=1.932 Giga-years Using the extrapolated procedure outlined in the main text, we get an age= 54.75 Mega-years. Lorentz and Gauss CSD ages are 8.51 Myr and 11.78 Myr respectively (cf. Table II) whereas Balan *et al.*^{S4} estimated it around 23.9 Mega-years.

The third example is drawn from Jonas^{S5} who worked extensively on fossil tooth enamel dating (spanning several hundred thousand years up to 2 Mega-years).

From the EPR lineshape (calibrated spectrum of fig.7), we extract the absorption line according to the above protocol with the result displayed in fig. S4.

We find the CSD between a Lorentzian (resp. Gaussian) $p(x)$ and Jonas^{S5} based $q(x)$ as 1.49×10^{-2} and 1.17×10^{-2} yielding respective ages 7.29 Kyr and 14.47 Kyr.

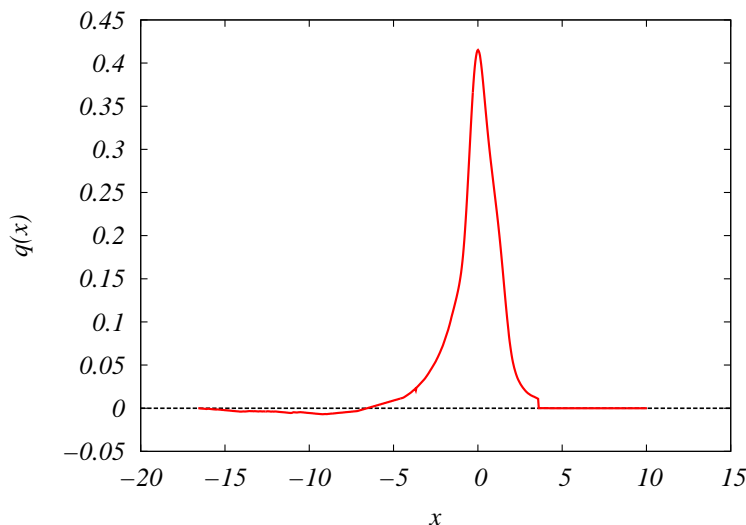


FIG. S4. (Color on-line) absorption line obtained from the fossil tooth enamel EPR lineshape of Jonas^{S5} fig.7. The negative part of the pdf is treated as in the B4 sediment case.

For the sake of comparison, if we use the $R_{10} = -3.26$ value (not to be used for the tooth enamel era but for ancient carbonaceous matter as in Bourbin *et al.*^{S6}), we get an age of 3.84 Gyr or an interpolated age of 97.08 Myr.

[S1]T. M. Cover, J. A. Thomas, "Elements of Information Theory" (John Wiley and Sons) (1991)

[S2]A. Skrzypczak, PhD Thesis, Université Paris VI (2005).

[S3]W.H. Press, S.A. Teukolsky, W.T. Vetterling and B.P. Flannery, "Section 14.7.2. Kullback-Leibler Distance". Numerical Recipes: The Art of Scientific Computing (3rd ed.), Cambridge University Press (2007).

[S4]E. Balan, T. Allard, E. Fritsch, M. Sélo, C. Falguères, F. Chabaux, M-C. Pierret and G. Calas, Formation and evolution of lateritic profiles in the middle Amazon basin: Insights from radiation-induced defects in kaolinite, *Geochimica et Cosmochimica Acta*, **69**, No. 9, 2193 (2005).

[S5]M. Jonas, Concepts and Methods of ESR dating, *Radiation Measurements*, Elsevier, **27**, 943 (1997).

[S6]M. Bourbin, D. Gourier, S. Derenne, L. Binet, Y. Le Du, F. Westall, B. Kremer and P. Gautret: Dating carbonaceous matter in archean cherts by electron paramagnetic resonance, *Astrobiology* **13-2**, 151 (2013).